JOURNAL OF CHEMICAL & ENGINEERING DATA

ARTICLE

pubs.acs.org/jced

Activated Neem Leaf: A Novel Adsorbent for the Removal of Phenol, 4-Nitrophenol, and 4-Chlorophenol from Aqueous Solutions

M. Ahmaruzzaman* and S. Laxmi Gayatri

Department of Chemistry, National Institute of Technology, Silchar, Assam-788010, India

ABSTRACT: The adsorption of three phenolic compounds, phenol (P), 4-nitrophenol (4-NP), and 4-chlorophenol (4-CP), on activated neem leaves (ANL) was investigated from simulated wastewater in batch as well as fixed bed mode. The effect of various operating parameters on adsorption such as adsorbent dose, solution pH, contact time, and temperature effect was monitored, and optimal experimental conditions were determined. The Langmuir, Freundlich, Redlich−Peterson, Dubunin−Radushkevich, and Temkin models were applied to describe the adsorption isotherms in the three systems. The goodness of curve fitting in the various models was done in accordance with linear regression coefficients and various error functions. Thermodynamic parameters such as the Gibbs free energy change, enthalpy change, and entropy change of the adsorption processes were also evaluated for the three different phenolic systems. The thermodynamic study shows the exothermic nature of the adsorption. The pseudofirst-order, pseudosecond-order, and Elovich equations were used to describe the kinetics of the adsorption processes. The pseudosecond-order model described the data very well ($R^2 > 0.99$). A comparative study of the batch adsorption with fixed bed adsorption was also conducted. Column studies showed a higher efficiency of the adsorbent than in the batch mode. The order of the adsorption capacity of ANL from the batch study was found to be 4-NP > 4-CP > P. In all cases the experimental data showed a good fit with the Freundlich equation. The calculated adsorption capacity proved the feasibility of using ANL as a potential adsorbent for the treatment of water containing 4-NP, 4-CP, and P.

1. INTRODUCTION

The purpose of this work was to investigate the efficiency of activated neem leaves (ANL) as an adsorbent for removal of three phenolic compounds, namely, phenol (P), 4-nitrophenol (4-NP), and 4-chlorophenol (4-CP) in aqueous solution. Phenols (1-hydroxybenzene) are the most prevalent form of pollutants in the chemical industry. Their presence is detected by bad taste and odor.[1] Phenols are considered as priority pollutants since they are harmful to organisms even at low concentrations. They are widely used as disinfectants for industrial and medical applications. Phenol also serves as a chemical intermediate for the manufacture of nylon-6 and other man-made fibers and for the manufacturing of epoxy and other resins and as a solvent for petroleum refining.

Phenolic compounds pose potential harm to human health and the environment, and they must be removed before being discharged into receiving waters. There has been an extensive study on the removal of phenolic compounds including 4-NP and 4-CP.[2−4] Technologies like biological degradation,[5] chemical oxidation,[6] and adsorption are constantly developing and being researched for the treatment of phenolic wastewater at high concentrations. Adsorption is considered to be an effective, low cost, and most frequently used method for the removal of phenolic compounds. The adsorption technique of water reclamation is superior in terms of initial cost, flexibility and simplicity of design, ease of operation, and insensitivity to toxic pollutants.[7] Although activated carbon is no doubt a superior adsorbent owing to its high adsorption capacity and porosity, the development of alternative adsorbents still continues as activated carbon is expensive and difficult to regenerate. Some of the adsorbents that have been studied include bentonite for the removal of chloro- and nitrophenols.[8,9] Recently, polymeric adsorbents, due to their more varied functionality, surface area, and porosity,[10,11] have been employed to remove phenolic compounds from aqueous solutions.[12−16] However, their wide scale application is hindered on the grounds of economic considerations.

Neem (*Azadirachta indica*) leaves were selected in the present study as they are easily available, fast growing, and widely cultivated, with as many as 14 million trees growing in India alone. Due to its multipurpose application in medicine as well as in cosmetics, it is widely grown with minimal or no maintenance in the tropical region. The leaves of the plant pile up as waste during defoliation and can be collected for use as an adsorbent. The adsorbent used for the present study was mainly carbonaceous in nature which was prepared by acid treatment of properly washed and dried neem leaves. In previous investigations, neem leaf powder was used for the removal of dyes like methylene blue[17] and brilliant green,[18] but no such study on the utilization of neem leaves for removal of phenolic compounds is known to the best of our knowledge. The focus of this work was to quantify the adsorption of three different types of phenolic compounds: 4-NP, 4-CP, and P on ANL using both a batch method as well as a fixed bed method and to determine the role of various parameters like media pH, contact time, and temperature on the equilibrium.

2. EXPERIMENTAL SECTION

2.1. Materials. The adsorbates selected for the adsorption study were P, 4-CP, and 4-NP. Solutions of the phenols were

Received: September 15, 2010
Accepted: April 15, 2011
Published: May 16, 2011

prepared by weighing out the pure crystalline solid. Neem leaves were obtained from waste piles of cultivation areas in northeastern India.

2.2. Preparation and Characterization of the Adsorbent. The ANL used in this present study was prepared by chemical activation of dried neem leaves using phosphoric acid in the ratio of 1:1 at 373 K for 2 h followed by heat treatment at 773 K for 3 h and frequently washed with distilled water to remove any free acids that may be present on the adsorbent surface until the pH reached ~6 to 7. The purpose of activation is to enhance the adsorption efficiency besides carbonizing the leaf material without the evolution of huge amounts of fumes as in the case of a physical method. The final product was then kept in an oven for 12 h at a temperature of (373 to 353) K to remove the excess moisture trapped inside the pores of the adsorbent. The ANL was then stored in a desiccator prior to its use. Scanning electron micrograph (SEM) analysis was performed to understand the morphology of the adsorbent. The surface chemistry of the prepared adsorbent (ANL) is governed by the presence of elements like nitrogen, hydrogen, sulfur, oxygen, and so forth, and the amount of which is further dependent on the mode of preparation, nature of the activating reagent, treatment conditions, and so forth. CHNOS analysis will determine the presence of these heteroatoms which are derived either from the precursor or during the treatment. The presence of these groups results in the acid/base character of ANL which is basically a carbon surface. The determination of surface functionality is of fundamental importance which can be studied from detailed Fourier transform infrared (FTIR) analysis of the adsorbent before and after adsorption. The surface chemistry of the carbon surface is best studied by a Boehm titration[19] which will identify the surface oxygenated groups. This is important as neither the surface area nor the pore structure study is sufficient enough to explain the properties of adsorption by the carbon surface.

2.3. Methods and Analysis. The test solutions were prepared by diluting stock solutions of 1000 $mg \cdot L^{-1}$ with double-distilled water. A total of 20 mL of the individual phenol samples containing ANL in varying weights from (0.1 to 1) g in different well-capped 100 mL flasks were kept in a constant temperature water-bath at specific temperatures maintained at (298, 308, and 318) K, and upon attainment of equilibrium, the supernatant liquid phase was characterized for absorbance at λ_{max} = 269 nm for P, 280 nm for 4-CP, and 315 nm for 4-NP using a Cary 100 Bio UV−vis spectrophotometer. The suspension was shaken at 150 rpm for uniform mixing of the adsorbate with the adsorbent for the first 12 h. In all cases, the initial pH of the solution was maintained at the natural pH of the solution. The adsorption isotherms were determined using both a column and batch equilibration technique. Batch equilibrium studies were carried out to find the optimum pH, contact time, and equilibrium isotherm. The amount of phenol adsorbed at equilibrium was calculated by the mass balance equation given by eq 1

$$q_e = \frac{V(C_o - C_e)}{m \cdot 100} \quad (1)$$

where q_e ($mg \cdot g^{-1}$) is the quantity of the adsorbate per unit mass of the adsorbent at equilibrium, V (mL) is the volume of the adsorbate, C_o ($mg \cdot L^{-1}$) is the initial liquid phase adsorbate concentration, C_e ($mg \cdot L^{-1}$) is the equilibrium liquid phase concentration, and m (g) is the mass of ANL.

2.4. Effect of Solution pH. The effect of initial pH on adsorption was studied by adjusting the solution pH in the range 2 to 12 using 0.1 M NaOH and 0.1 M HCl solutions. In these experiments the ANL loading was maintained at 10 $g \cdot L^{-1}$ of the respective phenol solution at 298 K. The contact time was kept as 48 h which is believed to be sufficient enough to reach equilibrium.

2.5. Kinetic Investigation. The kinetic experiments were conducted at 298 K in a standardized batch adsorber which consisted of several 100 mL glass capped Erlenmeyer flasks containing different phenol solutions (20 mL each) kept in contact with 0.2 g of ANL and placed inside the reactor by stirring at 150 rpm. The samples were withdrawn at definite time intervals and analyzed for the respective phenol concentration.

2.6. Determination of pH_{ZPC}. pH_{ZPC} is the pH when the charge on the ANL surface is zero. The pH drift method[20] was used to determine the pH_{ZPC} of the ANL carbon surface using 50 mL of 0.1 M NaCl in a series of Erlenmeyer flasks whose pH values were adjusted using 0.1 M NaOH and 0.1 M HCl in the range between 2 and 12. The initial pH of the solutions was determined, and 0.15 g of the adsorbent was added to each of the flasks; after completion of 48 h, the final pH of the solutions was measured. The pH_{ZPC} was noted at the pH at which the initial pH equals the final pH.

2.7. Column Studies. Fixed bed studies were conducted in a fixed bed of down flow, 4.3 cm in diameter and 60 cm in length for the glass columns. Breakthrough capacity was determined by taking 1000 $mg \cdot L^{-1}$ of feed solution containing the particular phenolic compound and passing it through the column containing 4 g of ANL, maintaining a flow rate of 2 $mL \cdot min^{-1}$. Prior to packing the column, a cotton plug was provided at the bottom to support the ANL bed as well as to prevent the washing out of the adsorbent. Another cotton plug was provided on the top of the bed to prevent floating up of the adsorbent during loading of the feed solution so as to maintain a fixed bed. To ensure complete expulsion of trapped air, the columns were wetted by passing double-distilled water prior to starting the experiment. The treated solutions were collected from the bottom portion after passing through different glass columns for different phenol systems and analyzed for P, 4-NP, and 4-CP concentrations at various time intervals. The process was continued until the amount of the particular phenol concentration was found to be same in the feed and the effluent. The breakthrough capacity was calculated using the ratio C_t/C_o, where C_t is the concentration of the phenolic compound in the effluent at time t and C_o is the concentration of the individual phenolic compound in the feed.

2.8. Desorption Studies. Desorption and regeneration studies are important in the field of adsorption studies. The desorption of an adsorbate loaded adsorbent was carried out by using 20 mL of various strengths of NaOH [(0.001 to 0.3) M], HNO_3 [(0.001 to 0.3) M], and water by taking 0.2 g of ANL preadsorbed with 20 mL of 1000 $mg \cdot L^{-1}$ phenol stock solution and stirring continuously at 150 rpm for 2 h. The desorption efficiency was calculated using the following equation:

$$\%\text{desorption} = \frac{C_d \cdot V_d}{w \cdot q_e \cdot 1000} \cdot 100 \quad (2)$$

where C_d ($mg \cdot L^{-1}$) is the desorbed adsorbate concentration, V_d (mL) is the volume of the desorption solution, and w (g) is the mass of the preadsorbed adsorbent.

Table 1. Characteristics of ANL

	value
Proximate Analysis of ANL	
moisture content	0.68 %
ash content	2.95 %
volatile matter content	1.05 %
fixed carbon content	95.32 %
Microanalysis Report for ANL	
carbon	60.9 %
nitrogen	5.57 %
hydrogen	3.83 %
Functional Groups	
carboxylic acid	3.287 $\mu g \cdot mol^{-1}$
lactone/lactol	0.322 $\mu g \cdot mol^{-1}$
phenolic	0.472 $\mu g \cdot mol^{-1}$
Chemical Parameters	
pH of the aqueous solution	2.99
pH_{ZPC}	2.2
BET surface area	890.45 $m^2 \cdot g^{-1}$
total pore volume	0.8895 $mL \cdot g^{-1}$

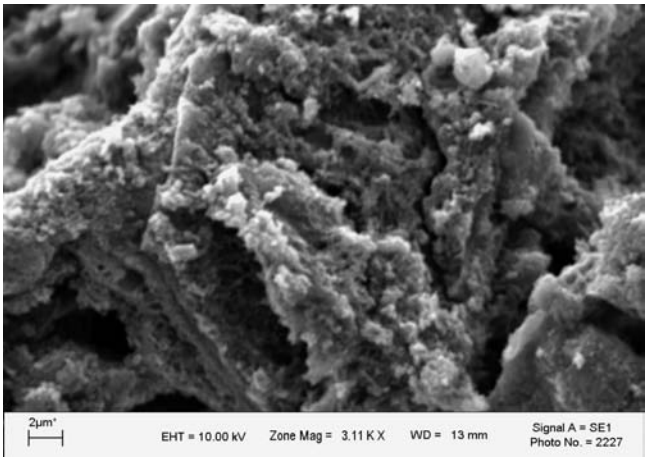

Figure 1. SEM image of ANL.

3. RESULTS AND DISCUSSION

3.1. Characterization of the Adsorbent. Since ANL is mainly a carbon material, the investigation of its surface topography with SEM and surface chemistry with an elemental analyzer play an important role in determining the adsorption properties. Some physical and chemical characteristics of the adsorbent is given in Table 1. The adsorption properties may also be ascribed from the low ash and high carbon content of ANL as depicted from proximate analysis data. Figure 1 reveals a SEM photomicrograph of ANL which depicts a highly heterogeneous surface with randomly oriented pits of several sizes along with some flaky particles. A FTIR study can provide useful qualitative information about the surface functionality. Figure 2a shows the FTIR spectrum of ANL before adsorption, while Figure 2 (b, c, and d) shows FTIR spectra of ANL after the adsorption of 4-NP, 4-CP, and P, respectively. Surface oxygen groups impart acidic character to the adsorbent surface, thereby affecting the nature of adsorption. The presence of such groups are indicated by the absorption bands at (3427.3, 1745.5, and 1180.3) cm^{-1}, which represent OH, ArC═O, and C—O stretching vibrations, respectively. The peak position at 3427.3 cm^{-1} has become less intense and has shifted to 3402.2 cm^{-1} after the adsorption of 4-NP. This region has been assigned to O—H stretching of the phenolic group. The bands at (1593.1 and 1570.0) cm^{-1} are attributed to NH_2 scissoring vibrations, which after adsorption of 4-NP appears as a single sharp peak at 1587.3 cm^{-1}, thereby proving the NH_2 groups are also responsible for the adsorption of 4-NP. After adsorption of 4-NP, the C—C═C asymmetric stretching of the aromatic ring has now shifted to 1587.3 cm^{-1} and 1465.8 cm^{-1} with increased intensity. It can be inferred that the alkane groups do not play any significant role in adsorption as their peak position at (2923.9 and 2852.5) cm^{-1} remain unchanged after adsorption. The C═O stretching of the ketonic group at 1745.5 cm^{-1} is found to be absent after adsorption of 4-NP, instead a new peak at 1720.4 cm^{-1} due to C═O stretching of the carboxylic group appears. The FTIR spectra after adsorption of 4-NP also shows a change in position and intensity of the C═O stretching of ethers at (1222.8, 1188.1, 1095.5, 1078.1, and 1058.9) cm^{-1}. The new peak position appearing at 1317.3 cm^{-1} is due to N═O bending of the nitro group which also confirms the adsorption of 4-NP onto ANL. The shifting of the peak position from 3427.3 cm^{-1} to 3415.7 cm^{-1} after the adsorption of P can explain the involvement of the H bonded −OH stretch in the adsorption of phenol. This band becomes broader and less intense after P adsorption. The band at 1745.5 cm^{-1} also becomes broader and decreases in intensity after adsorption of P showing the possible participation of the carboxylic group toward P adsorption. Changes also appear in the carboxylate band which now appears at 1589.2 cm^{-1}. The peak at 692.4 cm^{-1} has shifted to 673.1 cm^{-1} due to the monosubstitution of the phenyl group. The ANL surface after 4-CP adsorption also shows shifting of −OH stretch to 3408.0 cm^{-1} along with broadening of the peak showing the possible role of this group in adsorption. The methylene band at 2923.9 cm^{-1} almost disappears, and the carboxylate peak (1587.3 cm^{-1}) shows significant decrease in intensity which reveals possible participation of this group in the adsorption of phenolic groups on the whole. The interaction of the phenyl aromatic ring can be interpreted from C—H in-plane aromatic bending becoming less prominent (broadening) at 1211.2 cm^{-1}. The spectra also reveals the presence of an alkyne C—H bending peak at 671.2 cm^{-1}.

3.2. Adsorption Equilibrium. In this study, the Langmuir, Freundlich, Temkin, Dubunin−Radushkevich, and Redlich−Peterson isotherm models were used to describe the equilibrium adsorption data. The different equilibrium adsorption isotherms[21−25] used to investigate the experimental data are given in Table 2. To optimize the design of the adsorption system, it is important to establish the most appropriate correlation for the equilibrium curves. Since each model has its own set of advantages and inconveniences, a detailed error analysis was undertaken to investigate the best fit adsorption isotherm which describes the adsorption process. The five different error functions[26] that were studied are listed in Table 3. The Langmuir isotherm model is one of the most common adsorption models, and it assumes monolayer coverage of adsorbate over a homogeneous adsorbent surface; at equilibrium, a saturation point is reached where no further adsorption can occur. The essential characteristics and feasibility of the Langmuir isotherm is

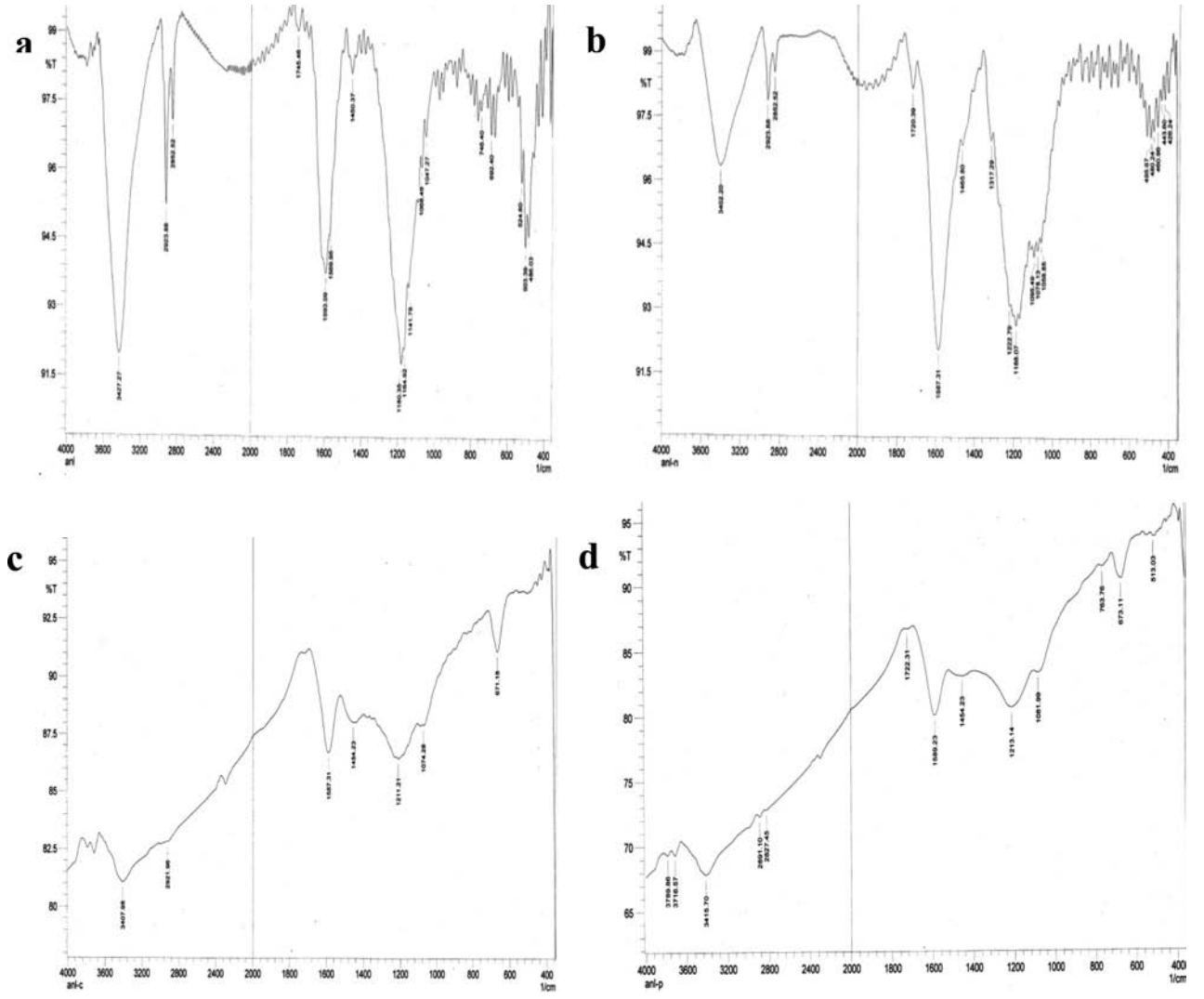

Figure 2. FTIR spectra of ANL; a, before adsorption; b, after adsorption of 4-NP; c, after adsorption of 4-CP, and d, after adsorption of P.

described in terms of a dimensionless constant separation factor (R_L), which is defined as:

$$R_L = \frac{1}{(1 + bC_o)} \quad (3)$$

If R_L value lies in between 1 and 0, favorable adsorption is indicated;[27] if greater than 1, unfavorable adsorption, while a value of 1 and 0 represents unfavorable and irreversible isotherms, respectively. The adsorption data obtained at 298 K represent favorable adsorption in the case of 4-NP, 4-CP, and P as the value of R_L turns out to be 0.085, 0.454, and 0.342, respectively. An attempt was also made to interpret the data using the Langmuir equation. However, the fit was typically found to be very poor (Table 4). The Freundlich isotherm is an empirical equation employed to describe heterogeneous systems. The constant K_F in the Freundlich expression is given in Table 2 is related to the capacity of the adsorbent for the adsorbate; $1/n_F$ is a function of the strength of adsorption. The Redlich−Peterson isotherm, on the other hand, is a three-parameter model which compromises the Langmuir model and the Freundlich model. The Redlich−Peterson isotherm constant, K_R, was obtained by maximizing R^2 using the computer program MATLAB while β and a_R are determined from the slope and the intercept of the linearized plot of the Redlich−Peterson equation (Table 6). Theoretically, the Redlich−Peterson isotherm approaches the Langmuir model if β equals unity. However, as seen from Table 6, it is clear that β is not equivalent to 1 and that the isotherm cannot be described by the Langmuir model. Though the R^2 value obtained from the Redlich−Peterson model in the case of 4-NP (value of 0.895 in Table 6) is higher than that of the Freundlich model (value of 0.862 in Table 5) at 298 K, the R^2 value in the overall range of temperature studied together with the values of error determined showed better fitting of the experimental data by the Freundlich adsorption isotherm. The Temkin adsorption isotherm assumes a uniform distribution of adsorption energies up to some maximum binding energy. The values of the Temkin constant along with the coefficient of determination and error data are reported in Table 7. It may be concluded that the Temkin isotherm does not represent the equilibrium data satisfactorily. The Dubinin−Radushkevich isotherm is one of the most widely used isotherm equations in the characterization of pore structure and description of the micropore filling process in microporous adsorbents. This model showed little or no fitting as depicted by Table 8 (low R^2 value and high error values).

Table 2. Isotherms and Their Linearized Expressions[a]

Sl. no.	isotherms	linearized equation	parameters
1	Langmuir[21]	$\frac{C_e}{q_e} = \frac{1}{a_L b_L} + \frac{C_e}{a_L}$	a_L, b
2	Freundlich[22]	$\log q_e = \log K_F + \frac{1}{n_F}\log C_e$	n_F, K_F
3	Temkin[b,23]	$q_e = B \ln K_{Tem} + B \ln C_e$	B, K_{Tem}
4	Dubunin−Radushkevich[24]	$\ln q_e = \ln \phi_D - \psi_D \left(\ln\left[1 + \frac{1}{C_e}\right]\right)^2$	ϕ_D, ψ_D
5	Redlich−Peterson[25]	$\ln\left[\frac{K_R C_e}{q_e} - 1\right] = \ln a_R + \beta \ln C_e$	K_R, a_R, β

[a] Here, a_L ($mg \cdot g^{-1}$) = monolayer adsorption capacity, a_R ($L \cdot mg^{-1}$) = Redlich−Peterson isotherm constant, b_L ($L \cdot g^{-1}$) = Langmuir isotherm constant, B = Temkin isotherm constant corresponding to the heat of adsorption, K_F ($mg \cdot g^{-1}$)($L \cdot mg^{-1}$)$^{1/n}$ = Freundlich adsorption coefficient, K_R ($L \cdot mg^{-1}$) = Redlich−Peterson isotherm constant, K_{Tem} ($L \cdot mol^{-1}$) = the equilibrium binding constant, β = constant of the Redlich−Peterson isotherm ($0 < \beta < 1$), ϕ_D ($mg \cdot g^{-1}$) = adjustable parameter in the Dubunin−Radushkevich equation, and ψ_D = adjustable parameter in the Dubunin−Radushvevich equation. [b] $B = (RT/b_T)$.

Table 3. Explanation of Different Error Functions[a]

error function	definition/expression
sum of the squares of errors (ERRSQ)[26]	$\sum_{i=1}^{p} (q_{e,cal} - q_{e,meas})_i^2$
hybrid fractional error function (HYBRID)[26]	$\frac{100}{p-n}\sum_{i=1}^{p}\left[\frac{(q_{e,meas} - q_{e,cal})^2}{q_{e,meas}}\right]_i$
Marquardt's percent standard deviation (MPSD)[26]	$100\left(\sqrt{\frac{1}{p-n}\sum_{i=1}^{p}\left[\frac{q_{e,meas} - q_{e,cal}}{q_{e,meas}}\right]_i^2}\right)$
average relative error (ARE)[26]	$\frac{100}{p}\sum_{i=1}^{p}\left\lvert\frac{(q_{e,cal} - q_{e,meas})}{q_{e,meas}}\right\rvert_i$
sum of absolute errors (EABS)[26]	$\sum_{i=1}^{p} \lvert q_{e,cal} - q_{e,meas}\rvert_i$

[a] Here, n = number of parameters of the isotherm equation, P = number of data points, $q_{e,cal}$ ($mg \cdot g^{-1}$) = calculated equilibrium solid phase concentration, and $q_{e,mass}$ ($mg \cdot g^{-1}$) = measured equilibrium solid phase concentration.

Figure 3 depicts the adsorption isotherm for 4-NP, 4-CP, and P (C_e versus q_e) at three different temperatures [(298, 308, and 318) K]. The isotherms follow the nature of IUPAC classification Type II describing adsorption on macroporous adsorbents with strong adsorbate−adsorbent interaction. In case of P and 4-CP, steps are present at low temperatures, but increasing temperature transforms them into smooth monotonic curves. It can further be followed from the shape of the adsorption isotherm that the density of functional groups present on the ANL surface is high. It was found that the percentage of adsorption increases with an increase in dosage of ANL which can be attributed to the increase in surface area and availability of more adsorption sites.

The removal of phenol is favorable at lower temperatures and decreases with an increase in temperature. A brief comparison of the uptake of the three phenolic compounds by ANL at 298 K is presented in Figure 4. It can be inferred that the adsorption capacity, q_e, increases with increasing equilibrium phenol concentrations. A steep rise in the adsorption is observed in case of 4-NP compared to that of 4-CP and P. The order of affinity of ANL toward the three phenols as seen from Figure 4 is P < 4-CP < 4-NP. The order remains the same irrespective of the temperature under study, though at higher equilibrium concentrations a change in the order is observed for 4-NP. This order seems to be related to the electron-withdrawing properties of the substituents of the phenolic compound. Therefore, electron withdrawal or deactivation of the benzene ring favors the formation of electron-donor−acceptor complexes between these rings and active groups on the surface of the ANL, increasing the adsorption capacity. The same trend for the adsorption of phenols on various adsorbents has been reported in the literature.[28]

On the basis of the lowest value of various error functions calculated and from the coefficient of determination, R^2 value, that is, the isotherm giving the R^2 value closest to unity, the fitting is Langmuir < Dubunin−Radushkevich < Temkin < Redlich−Peterson < Freundlich. The nature of the adsorption isotherm curve showing a Type II isotherm which predicts the adsorption for macroporous adsorbents as shown in Figure 4 clearly indicates that the Langmuir model and Dubunin−Radushkevich model cannot be used to describe the adsorption process. A comparison of the experimental adsorption data with the linearized plot of the Langmuir, Freundlich, Temkin, Dubunin−Radushkevich, and Redlich−Peterson models is shown in Figure 5 for the different phenol systems. It shows that none of the isotherm models used in the study could sufficiently describe the equilibrium adsorption data for 4-NP (Figure 5c). However, a close examination of the linear isotherm plots and from the R^2 value along with the error analysis suggested that the Freundlich isotherm model yielded a much better fit than the other models.

3.3. Effect of pH on Adsorption and pH_{ZPC}. The presence of several functional groups introduces acidic/basic character to the adsorbent surface and causes the surface properties of ANL to depend on the pH of the aqueous solution. The pH of the adsorbate solution is an important parameter governing the adsorption of phenolic compounds on various adsorbents. Chlorophenols are weak acids in aqueous solutions; they exist primarily in the molecular form under acidic conditions while the anion predominates at neutral or basic pH. Phenol is a weak aromatic acid. The surface of ANL is negatively charged[29] at the pH above the pH_{ZPC}. The drift method was used to measure the pH_{ZPC} of

Table 4. Langmuir Isotherm Constants at Different Temperatures for Different Phenolic Systems on ANL

	temperature (K)	a_L mg·g^{-1}	b_L L·g^{-1}	R_L	R^2	SD	ERRSQ	HYBRID	MPSD	ARE	EABS
4-NP	298	1000	0.010	0.085	0.484	0.086	55400.17	9332.03	64.997	16.297	267.483
	308	1000	0.006	0.129	0.278	0.068	319003.75	40468.36	34.813	1.392	28.923
	318	1000	0.007	0.119	0.302	0.069	373856.10	45567.54	40.902	3.625	2.097
4-CP	298	500	0.001	0.454	0.803	0.290	145705.30	23477.29	15.158	7.49	60.547
	308	166.6	0.004	0.197	0.980	0.246	64704.49	15058.05	5.960	0.625	1.811
	318	250	0.002	0.289	0.948	0.283	93068.58	18784.62	11.516	4.476	33.622
P	298	125	$1.91 \cdot 10^{-3}$	0.342	0.828	0.847	131.27	77.66	5.416	3.591	12.319
	308	416.66	$9.04 \cdot 10^{-4}$	0.525	0.997	0.337	3.693	3.959	3.582	1.434	2.263
	318	43.47	0.013	0.069	0.995	2.761	12.46	148.768	12.46	9.0883	17.989

Table 5. Freundlich Isotherm Constants at Different Temperatures for Different Phenolic Systems on ANL

	temperature (K)	n_F	K_F mg^{-1}·L$^{1/n}$·g^{-1}	R^2	SD	ERRSQ	HYBRID	MPSD	ARE	EABS
4-NP	298	2.17	41.129	0.862	0.153	13179.393	3414.7	34.118	3.341	90.682
	308	1.35	12.824	0.915	0.122	32431.049	2060.82	27.534	2.521	73.421
	318	1.42	16.107	0.909	0.129	44906.010	2585.31	29.057	2.631	91.615
4-CP	298	1.49	2.688	0.981	0.032	740.589	96.027	7.3118	0.324	8.125
	308	2.35	7.726	0.985	0.018	85.867	19.547	4.225	0.467	3.512
	318	1.87	4.609	0.962	0.035	349.322	71.411	7.754	0.282	4.125
P	298	1.798	1.761	0.945	0.040	65.511	33.359	2.1605	0.1504	3.013
	308	1.35	12.823	0.915	0.337	3.9431	4.2070	3.677	0.261	0.558
	318	4.69	9.749	0.965	0.013	219.415	164.829	13.856	4.828	14.042

Table 6. Redlich−Peterson Isotherm Constants at Different Temperatures for Different Phenolic Systems on ANL

	temperature (K)	K_R L·g^{-1}	a_R L·mg^{-1}	β	R^2	SD	ERRSQ	HYBRID	MPSD	ARE	EABS
4-NP	298	1714.8	40.812	0.543	0.895	0.357	43155.53	5154.87	25.392	3.986	83.953
	308	13.2	0.236	0.517	0.596	0.534	36557.66	3169.72	21.067	5.322	64.939
	318	12.75	0.062	0.809	0.710	0.694	60012.88	4741.686	29.24	7.389	90.314
4-CP	298	1.04	0.054	0.585	0.931	0.128	928.443	164.697	1.619	0.510	3.376
	308	1.45	0.061	0.728	0.993	0.047	82.638	25.188	0.402	0.465	2.137
	318	1.3	0.080	0.633	0.957	0.107	327.017	95.585	1.535	5.865	39.113
P	298	68.41	38.474	0.444	0.916	0.093	62.571	41.494	2.46	9.674	14.454
	308	0.21	$1.026 \cdot 10^{-2}$	1.225	0.994	0.047	2.172	7.066	0.162	1.992	3.267
	318	0.49	$2.92 \cdot 10^{-2}$	1.238	0.982	0.143	71.698	55.933	5.062	8.852	19.531

ANL whose value was determined to be 2.2. The adsorption of the phenol solutions was studied in natural unbuffered pH conditions to determine the equilibrium pH for maximum adsorption. It can be seen from Figure 6 that phenol uptake does not fluctuate with increasing pH after 11. It remains almost the same from pH 3 to 11. This is because phenol dissociates forming phenolate ions at a pH around 11 while the surface of ANL remains either neutral or negatively charged. The electrostatic repulsion between the phenolate ions and the negatively charged surface of ANL results in a decrease in adsorption capacity of phenol at pH above 11. However, the undissociated basic groups may still form some donor−acceptor kind of relation along with some dispersion interaction. For phenol, the acidic groups are responsible for the adsorption on ANL since the adsorption capacity is higher in high H^+ concentration. The adsorption capacity was high in the low pH range (1 to 4) after which pH has almost negligible effect on adsorption as the adsorption capacity remains almost constant. Considering the pH effect on 4-CP adsorption, it is important to note that the maximum adsorption for 4-CP adsorption takes place at pH 7.72. The behavior can be explained by considering the nature of the surface functional groups on the adsorbent at different pH values in 4-CP solution and also the behavior of the ionic state of 4-CP at these pH. There is also some partial contribution from electrostatic interaction between some of the positively charged surface functional groups and negatively charged chlorophenolate ions for the adsorption of 4-CP up to

Table 7. Temkin Isotherm Constants at Different Temperatures for Different Phenolic Systems on ANL

	temperature (K)	K_{Tem} L·g^{-1}	B	R^2	SD	ERRSQ	HYBRID	MPSD	ARE	EABS
4-NP	298	0.548	90.48	0.609	139.48	58366.95	8424.356	80.26	4.186	0.020
	308	0.170	131.9	0.696	109.46	47931.5	5191.437	61.936	15.218	0.519
	318	0.207	129.7	0.657	125.56	63067.47	6599.42	71.521	1.237	0.107
4-CP	298	0.018	77.97	0.903	20.67	1710.614	285.775	15.419	0.259	0.293
	308	0.037	37.56	0.974	4.98	99.581	23.786	4.898	0.052	0.110
	318	0.024	51.45	0.949	9.48	359.74	93.745	10.345	0.326	0.228
P	298	45.29	23.65	0.89	5.578	155.588	86.616	6.019	0.408	0.014
	308	0.398	6.30	0.898	1.081	3.51	3.787	3.509	0.072	0.-014
	318	0.465	6.727	0.959	1.078	196.229	147.473	12.40	7.504	13.832

Table 8. Dubunin−Radushkevich Isotherm Constants at Different Temperatures for Different Phenolic Systems on ANL

	temperature (K)	ϕ_D mg·g^{-1}	ψ_D	R^2	SD	ERRSQ	HYBRID	MPSD	ARE	EABS
4-NP	298	229.522	$1.11\cdot10^{-5}$	0.466	0.698	11973.86	11534.233	107.79	14.825	185.322
	308	236.275	$1.249\cdot10^{-5}$	0.640	0.582	95432.44	6972.327	77.68	11.235	170.437
	318	232.525	$7.1\cdot10^{-5}$	0.603	0.622	210486.693	6754.8	1628.435	154.529	530.529
4-CP	298	165.836	$1.933\cdot10^{-2}$	0.809	0.257	5142.318	778.874	11.289	1.806	20.997
	308	116.279	$1.590\cdot10^{-2}$	0.854	0.134	700.429	120.089	3.972	0.603	4.554
	318	132.82	$1.665\cdot10^{-2}$	0.803	0.192.	1613.12	410.823	9.199	1.258	10.209
P	298	50.199	$1.497\cdot10^{-2}$	0.634	0.241	648.92	256.583	13.279	2.051	7.661
	308	36.818	$2.881\cdot10^{-2}$	0.948	0.023	1.851	1.867	0.098	$8.8\cdot10^{-2}$	0.068
	318	33.0162	$3.151\cdot10^{-4}$	0.371	0.134	91.438	59.182	4.393	0.599	1.594

pH 7.72. As the pH shifts to a more basic range, the adsorption of 4-CP decreases gradually and then sharply at a pH above 12. This may be due to the fact that the ANL surface now contains functional groups with net negative charge which shows repulsion with the chlorophenolate ions at pH above 7.72. However, as some degree of adsorption is still present at pH above 7.72, the role of other mechanisms like physical adsorption might have taken place. In case of 4-NP the rate of removal is considerably reduced at a pH above 8.18 as it visible from the steep fall in adsorption capacity at pH > 8 in Figure 6. The adsorption capacity decreased dramatically when the solution pH varied from the acidic to alkaline range. 4-NP exists as the phenolate ion in the alkaline range, and it can be inferred from Figure 6 that hydrophobic interaction between the molecular form of 4-NP and ANL is responsible for the high adsorption capacity at low pH conditions. The hydrophilic nature of 4-NP under high alkaline conditions makes the situation difficult for 4-NP adsorption at high pH conditions.

3.4. Effect of Contact Time. The experiments were carried out with an adsorbent dosage of 0.2 g/20 mL of different phenol solutions at 298 K for different periods of contact time with the maximum reaching 24 h. The removal of P (Figure 7a), 4-CP (Figure 7b), and 4-NP (Figure 7c) increases with time and attains saturation in about 7 h. This indicates that the equilibrium contact time needed for 4-NP, 4-CP, and P adsorption was nearly 7 h in all three cases. Adsorption was rapid within the first 1 h and became almost asymptotic after 12 h. The decrease of adsorption rates is well-illustrated by the plateau line after 7 h of adsorption. Adsorption is rapid during the first 1 h due to the bulk diffusion from the solution to the surface of the adsorbent; it slows down after the first 1 h due to the change in adsorption mechanism and finally attains a plateau indicating the attainment of equilibrium.

3.5. Adsorption Kinetic Studies. The time-dependent batch adsorption data using a fixed dose of adsorbent (0.2 g) at 298 K was used for kinetic modeling of the different phenol systems with an initial concentration of 1000 mg·L^{-1}. The model equations that were used include: pseudofirst-order, pseudosecond-order, and Elovich equations. The contact-time study can be used to determine the rate-limiting step in the adsorption process with the help of a Weber−Morris plot. The possible rate-limiting steps are (i) mass-transfer from the bulk liquid to the particle external surface, (ii) film diffusion, and (iii) intraparticle diffusion.[30] The rate constant for intraparticle diffusion was evaluated using the equation below:

$$q_t = K_i t^{1/2} + C \quad (4)$$

where q_t (mg·g^{-1}) is the equilibrium solid phase concentration at time, t and C is a constant.

The values of diffusion coefficient, K_i, evaluated from the plots were (2.523, 0.121, and 0.784) mg·g^{-1}·h^{-1} for P, 4-NP, and 4-CP, respectively. The plot of square root of time versus adsorption capacity (plot not shown) does not pass through the origin indicating that intraparticle diffusion is involved but is not the rate-controlling step of the adsorption process in the case of P. This model does not show a good representation of the experimental data for 4-NP and 4-CP. The adsorption of 4-NP, 4-CP, and P on ANL cannot be explained by the first-order

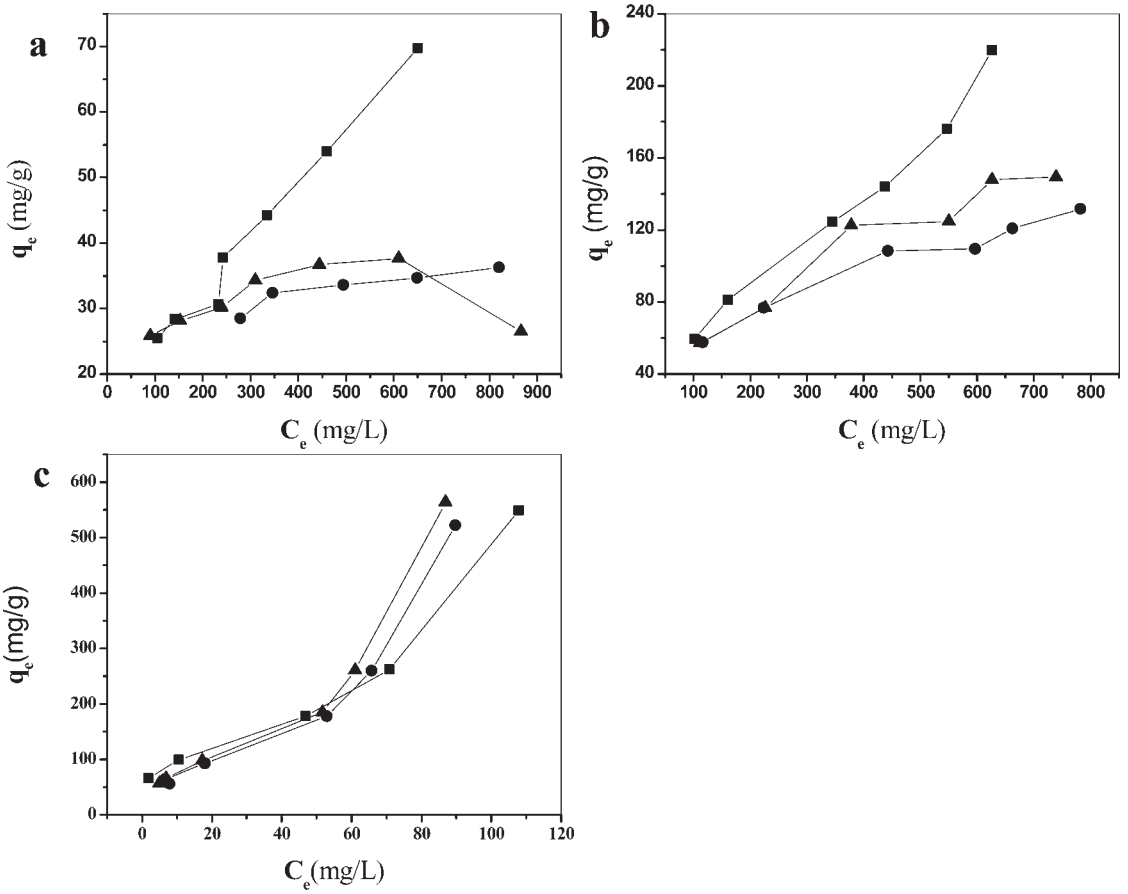

Figure 3. Adsorption isotherm for different phenol systems showing the effect of temperature: (a) P, (b) 4-CP, and (c) 4-NP (■, 298 K; ●, 308 K; ▲, 318 K).

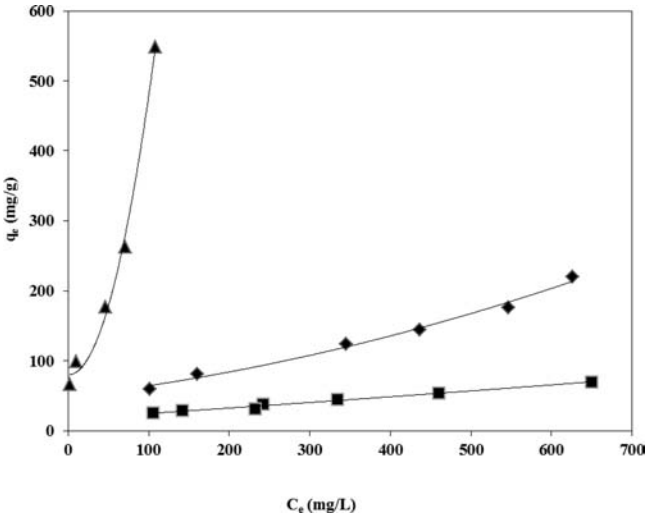

Figure 4. Comparison of adsorption isotherms for single phenol systems; conditions: C_o = 1000 mg·L^{-1}, T = 298 K (■, P; ▲, 4-NP; ♦, 4-CP).

reaction as can be seen from Table 9, and hence a detailed discussion on pseudofirst-order kinetic modeling is neglected.

The pseudosecond-order equation[31] based on the equilibrium adsorption is expressed as

$$\frac{t}{q_t} = \frac{1}{k_2 q_e^2} + \frac{1}{q_e} t \qquad (5)$$

The linear plot of t/q_t versus t can be used to determine q_e and k_2 from the slope and intercept of the plot. Here k_2 (g·mg^{-1}·h^{-1}) is the rate constant of pseudosecond-order adsorption.

Table 9 shows a good agreement between the experimental and the calculated q_e value from the pseudosecond-order rate equation. Besides, the coefficient of determination for the second-order kinetic model approaches 1, indicating the applicability of the second-order kinetic model to describe the adsorption process of 4-NP on ANL. The R^2 value for 4-CP and P were also high (0.999 and 0.998, respectively) with the pseudosecond-order model as compared to first-order and Elovich equations.

3.5.1. Validity of the Kinetic Model. The applicability of the kinetic model to describe the adsorption process was further validated by the normalized standard deviation, Δq%, which is defined as:

$$\Delta q(\%) = 100\sqrt{\frac{\sum[(q_{exp} - q_{cal})/q_{exp}]^2}{N-1}} \qquad (6)$$

where N is the number of data points and q_{exp} and q_{cal} (mg·g^{-1}) are the experimental and the calculated adsorption capacity, respectively. Table 9 list the $\Delta q(\%)$ values obtained for the three models tested.

3.6. Adsorption Mechanism. To understand the mode of interaction between the ANL surface and the three phenolic groups under investigation, the surface of the adsorbent has to be studied from a qualitative as well as quantitative point of view. The results of ultimate analysis showed the presence of various

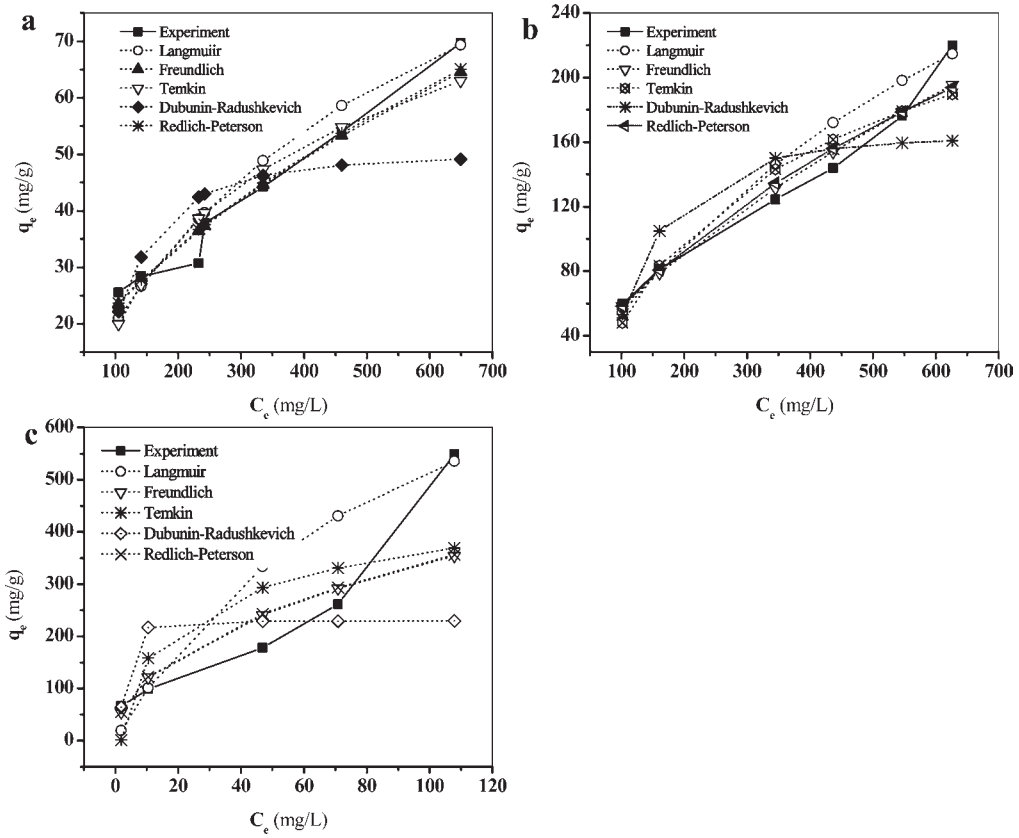

Figure 5. Validity of adsorption isotherm for the three phenol systems toward different adsorption models at 298 K: (a) P, (b) 4-CP, and (c) 4-NP; initial concentration = 1000 mg·L^{-1}.

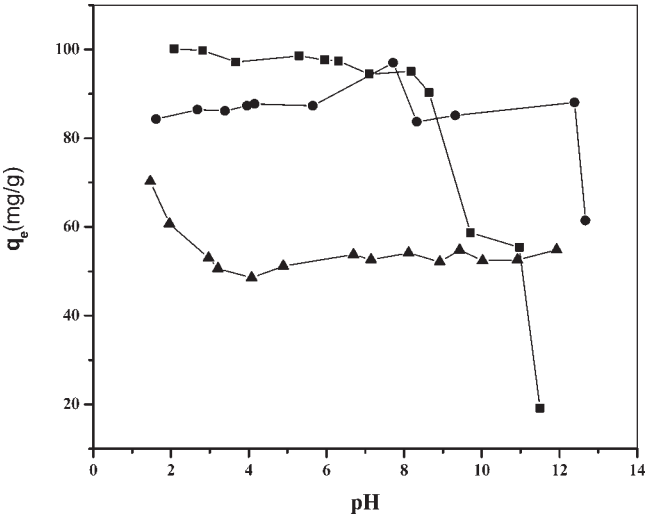

Figure 6. Effect of pH media on the adsorption of 4-NP, 4-CP, and P (■, 4-NP; ●, 4-CP; ▲, P).

atoms other than carbon itself. They are hydrogen, nitrogen, oxygen, and sulfur as given in Table 1, which may be present as heteroatoms on the aromatic ring or as functional groups like phenol, carboxyl, lactones, ether, nitro, amine, and so forth. The presence of these functional groups can further be confirmed from the FTIR study of the adsorbent before adsorption. If oxygen-containing groups are present, a basic character is imparted to the adsorbent surface. Groups such as OH, NH_2, OR, or O(C═O) are classified as electron donors (due to the presence of σ or π electrons), whereas (C═O) OH, (C═O) H, or NO_2 groups are classified as electron acceptors (due to the presence of empty orbitals). The possible interaction between the carbon surface of ANL and phenols is (a) a dispersion effect between the aromatic ring and the π electrons of the carbon structure of the adsorbent, (b) electrostatic interaction when ions are present, and (c) electron donor−acceptor interaction between the aromatic ring and basic surface sites. From the pH_{ZPC} determination, the functional groups on the carbon surface of ANL and phenolic compounds are in nonionized form at pH = 2.2. As deduced from q_e values for the adsorption of P, 4-NP, and 4-CP, the interaction between phenol and ANL is the weakest and may be attributed due to dispersion effects. The weak interaction also results from the competitive adsorption of phenol molecules with water molecules due to H-bonding of the electronegative surface oxygen atoms and water itself, yielding a smaller surface concentration for phenol molecules to adsorb. 4-CP exhibits a greater affinity for the ANL surface owing to the presence of the electron-withdrawing chlorine substituent. It may also be mentioned here that, since phenols have a strong hydroxyl functional group, interaction of the adsorbent surface also occurs through the hydroxyl group and additional adsorption occurs by the interaction between the adsorbed molecules. This phenomenon contributes significantly to the cooperative nature of adsorption and hence S type curves.[32]

3.7. Effect of Temperature and Thermodynamics Parameters. The effect of temperature on the adsorption of 4-NP, 4-CP, and P by ANL was studied at temperatures of (298, 308,

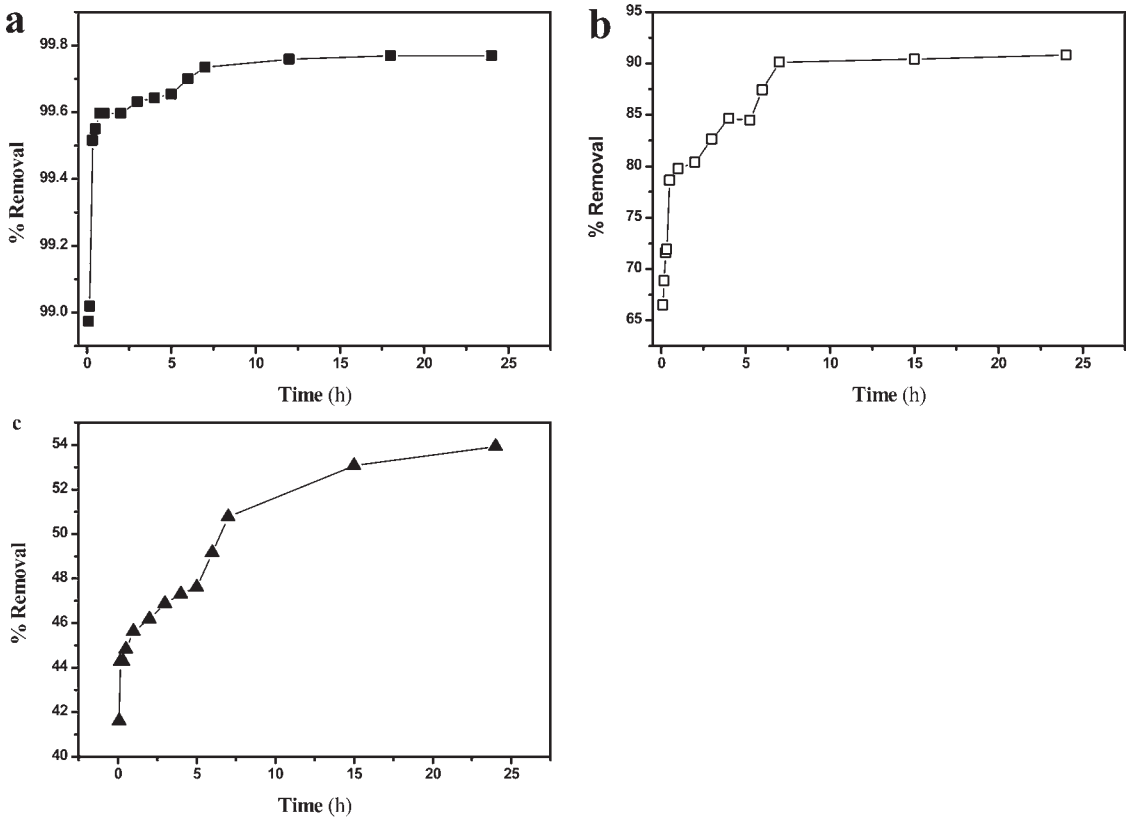

Figure 7. Effect of contact time on the adsorption of phenols (a) 4-NP, (b) 4-CP, and (c) P; ANL dosage = 10 g·L^{-1}, temperature = 298 K, C_o = 1000 mg·L^{-1}; (■, 4-NP; □, 4-CP; ▲, P).

Table 9. Kinetic Model Parameters for the Adsorption Process at 298 K[a]

model	system	parameters	R^2	$q_{e,cal}$ mg·g^{-1}	Δq%
Pseudofirst Order		k_1 (h^{-1})			
	4-NP	0.294	0.857	0.367	103.128
	4-CP	0.149	0.822	15.066	84.199
	P	0.112	0.894	9.66	82.75
Pseudosecond Order		k_2 (g·(mg·h)$^{-1}$)			
	4-NP	3.333	1	100	0.514
	4-CP	0.121	0.999	90.909	18.908
	P	0.064	0.998	55.55	20.602
Elovich		a b			
	4-NP	8.13	0.755	99.825	0.365
	4-CP	$4.54 \cdot 10^{-34}$ 4.761	0.959	−15.7826	83.269
	P	$5.086 \cdot 10^{-21}$ 2.192	0.882	−19.5	61.066

[a] Here, a and b refer to the Elovich constant, while the rest of parameters have been defined earlier.

and 318) K. The temperature study shows that the optimum adsorption takes place at 298 K. From thermodynamic data (negative value of ΔH), the exothermic nature of the adsorption process of the three phenolic compounds is evident. Figure 3a shows comparatively high adsorption capacity at 298 K than at (308 and 318) K, though the effect becomes less pronounced with the progress of adsorption. A similar behavior was also observed in the case of 4-CP adsorption (Figure 3b). A close examination of Figure 3c shows that at higher equilibrium 4-NP concentration, that is, at the initial stages of adsorption, an increase in temperature does not have a marked effect on the adsorption process. But as the adsorption proceeds the adsorption curve at 298 K emerges above that of (308 and 318) K proving 298 K as the optimum adsorption temperature. The Gibbs energy, enthalpy, and entropy (ΔG, ΔH, ΔS) for the adsorption process were obtained from the experiments carried out at different temperatures using the following equations.[33]

$$K_c = \frac{C_a}{C_e} \tag{7}$$

$$\Delta G^o = \Delta H^o - T\Delta S^o \tag{8}$$

where K_c is the equilibrium constant, C_e the equilibrium concentration in the solution (mg·L^{-1}), and C_a is the solid phase concentration at equilibrium (mg·L^{-1}), that is, the mass of phenol adsorbed by ANL at equilibrium. K_c is defined as the ratio of the amount adsorbed per unit mass to the solute concentration in the unit volume of the solution at equilibrium.

The thermodynamic parameters for the adsorption process (Table 10) were computed from the plot of ln K_c versus $1/T$. These values were used to calculate ΔG^o using eq 8. These plots showed a certain degree of linearity with coefficient of determination values varying from 0.874 to 0.976. The ΔH^0 values were negative for all three phenols, thereby conforming to the exothermic nature of the adsorption process. The similar exothermic nature for the adsorption of phenols on various

Table 10. Thermodynamic Parameters for Phenol Adsorption

	ΔH^0	ΔS^0	ΔG^0
phenol system	kJ·mol^{-1}	J·mol^{-1}·K^{-1}	kJ·mol^{-1}
4-NP	−203.304	−244.681	−130.389
4-CP	−73.218	−87.878	−99.406
P	−129.855	−172.598	−78.421

adsorbents has been reported in the literature.[28] The values of Gibbs energy changes are negative, confirming that the adsorption of the three different phenols on ANL was spontaneous and thermodynamically favorable. The more negative values of ΔG^0 implied that a greater driving force is required for the adsorption process. The negative values of ΔS^0 indicated a strong affinity of the adsorbate molecules by the ANL surface.

3.8. Desorption Studies. Desorption can take place either by thermal treatment or by use of a suitable desorbing agent. The highly acidic groups like carboxyl and lactones will be desorbed as CO_2 at (200 to 650) °C, while the less acidic (phenols, carbonyls) and the basic groups are desorbed mainly as CO or a mixture of CO and CO_2 in the range of (500 to 1000) °C.[34] However, the method of activation using phosphoric acid adopted for the preparation of the present adsorbent was performed under insignificantly high temperature (500 °C), and hence thermal desorption, that is, desorption at high temperatures is therefore not required. Figure 8 shows the desorption of three different kinds of phenol using different eluents at T = 298 K. The desorption efficiency was found to be highest (37.97 %) in case of 0.3 M NaOH for phenol (Figure 8), and hence 0.3 M NaOH can be used as regenerating agent for phenol from ANL. Though 0.3 M NaOH was found to be the best desorbing agent, the % desorption was lower (26.05 %) in case of 4-CP, while the maximum desorption (24.77 %) for 4-NP can be obtained using 0.3 M HNO_3.

3.9. Analysis of Column Data. A number of studies on the removal of phenolic compounds using a batch technique have been reported in the literature. However, for the practical operation on full-scale, a continuous flow fixed bed column is often preferred as it is easy to operate and attains a high yield. The time for the appearance of breakthrough and the shape of the breakthrough curve are important aspects in determining column efficiency. The position of the breakthrough curve along the time axis depends on the bed height, flow rate, and feed concentration. Through the column study, we can predict as to how much effluent can be treated by the bed and how long the bed will last before regeneration is necessary.

Column studies are used to assess the performance of the adsorbent tested on the bench-scale to pilot-scale testing. The dynamic behavior of the fixed bed column is described in terms of effluent concentration−time profiles which are also described as the breakthrough curve. The fixed bed study of phenol (Figure 9c) shows quantitative adsorption of phenol within a short contact time. To model the column operation, the bed-depth service time was applied to the adsorption data. After 41 h of continuous inflow of 4-NP, the adsorption capacity of the ANL-packed bed is almost exhausted as significant from the breakthrough curve given in Figure 9b, whereas, in the case of P and 4-CP, the adsorption capacity of the bed was exhausted much earlier, that is, after (10 and 14.4) h of operation (Figure 9a).

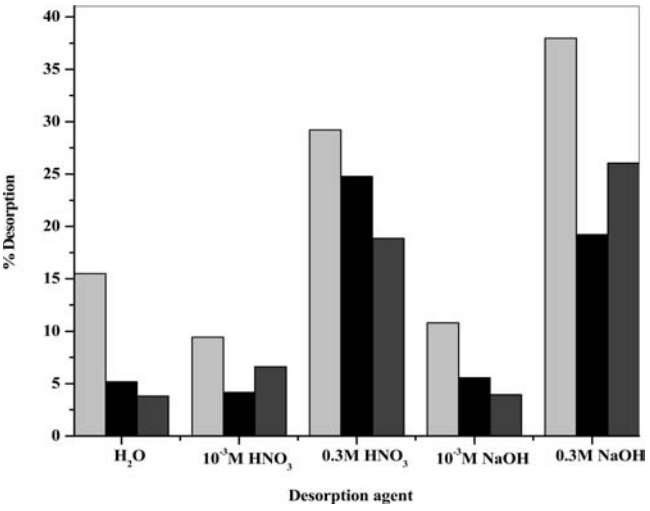

Figure 8. Desorption of adsorbate-loaded ANL with various eluent at T = 298 K using 0.1 g of the adsorbent (light gray, P; black, 4-NP; dark gray, 4-CP).

These results were achieved using a bed height of 2 cm and adsorbent loading of 4 g. There is a scope for further improvement of adsorption capacity and increased exhaustion time with an increase in the adsorbent loading mass. The breakthrough curve for 4-NP, P, and 4-CP shows favorable adsorption as there is an instantaneous jump in effluent concentration from zero to the feed concentration when the breakthrough point is reached.[35] The adsorption capacity of ANL was found to be higher using the fixed bed than found in the batch study. This is due to the fact that in a column operation the adsorbent is continuously in contact with a fresh solution, and hence, the concentration of the solution in contact with a given layer of adsorbent in the column is relatively constant.

The total adsorbed phenol (m_a) in the column for the initial feed concentration of 1000 mg·L^{-1} and the flow rate can be calculated mathematically using eq 9.[35]

$$m_a = \frac{Q.A}{1000} = \frac{Q}{1000}\int_{t=0}^{t=t_{tot}} C_{ad}.dt \qquad (9)$$

where Q is the volumetric flow rate in mL·min^{-1} and t_{tot} refers to the total flow time (min). The area under the breakthrough curve (A) is calculated by integrating the adsorbed concentration (C_{ad}) versus t plot using the Origin 6.1 software. The total amount of phenol fed through the column (m_{tot}) can be calculated using eq 10.

$$m_{tot} = \frac{C_0 \cdot Q \cdot t_{tot}}{1000} \qquad (10)$$

The total removal percentage is calculated from the ratio of the total adsorbed quantity of phenol to the total amount of the respective phenol feed (m_{tot}) to the column which is calculated using eq 11.

$$\text{total removal percentage} = \frac{m_a}{m_{tot}} \cdot 100 \qquad (11)$$

The equilibrium adsorption capacity (q_{eq}) for the respective phenol uptake from the column study is obtained from the ratio of the total adsorbed quantity (m_a) to the total mass of the adsorbent (W) feed in the column. The values of m_a, q_{eq}, and the

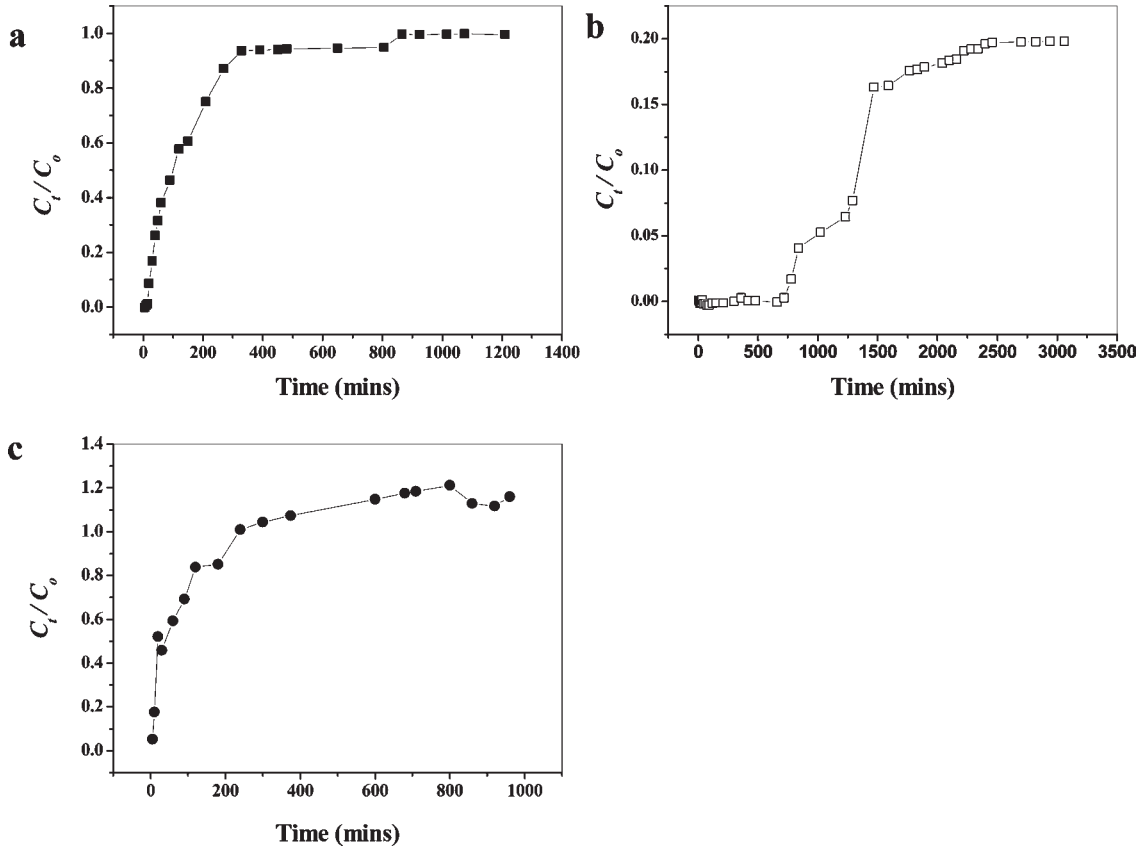

Figure 9. Breakthrough curves for ANL (a) 4-CP, (b) 4-NP, and (c) P; flow rate of 2 mL/min, initial concentration = 1000 mg·L^{-1}, amount of adsorbent loaded = 4 g, column height = 2 cm; (■, 4-CP; □, 4-NP; ●, P).

Table 11. Adsorption Data for Fixed Bed ANL Column for Different Phenol Systems[a]

	m_a		q_{eq}
phenol system	mg	% removal	mg·g^{-1}
4-NP	5428.86	88.71	1357.215
4-CP	320.06	13.22	80.015
P	48.02	2.50	12.01

[a] Process parameters: (bed depth = 2 cm, C_0 (mg·L^{-1}) = 1000 and Q = 2.0 mL·min^{-1}).

total removal percent of the particular phenol calculated from the column data are presented in Table 11.

4. CONCLUSIONS

The need for a cleaner environment demands adsorbents that meet the requirement of efficiency as well as being cheap and easily available in nature. The high adsorption capacity proved the effectiveness of ANL as a promising adsorbent for the removal of 4-NP, 4-CP, and P. The adsorption isotherms displayed the following order of adsorption capacity of ANL: P < 4-CP < 4-NP. In all cases the experimental data were well-fitted by the Freundlich equation obtained by assuming that the surface is heterogeneous with adsorption sites of different energy. It was found that the adsorption is a co-operative process due to association with the aromatic groups of phenol. An important operational variable in adsorption of phenols is temperature; that is, adsorption of P, 4-CP, and 4-NP is more favorable at low temperatures, the optimum being at 298 K under the experimental conditions investigated. The batch adsorption tests indicate that ANL had a notable adsorption capacity for the removal of P, 4-CP, and 4-NP from wastewater following pseudosecond-order kinetics. The advantage/effectiveness of column operation over batch study in the removal of phenolic compounds was also proved in this work. The present study may be helpful for designing treatment plants for water and wastewater bearing phenolic compounds.

■ AUTHOR INFORMATION

Corresponding Author

*E-mail: md_a2002@rediffmail.com.

■ ACKNOWLEDGMENT

The authors are thankful to the Central Instrumentation Facility (CIF), Indian Institute of Technology (IIT), Guwahati, for providing the scanning electron micrograph (SEM) analysis for the present study. We are also grateful to Chemical Engineering Department, IIT, Guwahati for providing us with surface area and porosity data of the adsorbent.

■ REFERENCES

(1) Patterson, J .W. *Wastewater Treatment Technology*; Ann Arbor Science: Ann Arbor, MI, 1997.

(2) Khan, A. R.; Ataullah, R.; Al-Haddad, A. Equilibrium Adsorption studies of some aromatic pollutants from dilute aqueous solutions on activated carbon at different temperatures. *J. Colloid Interface Sci.* **1997**, *194*, 154–165.
(3) Chern, J.-M.; Chein, Y. W. Adsorption of nitrophenol onto activated carbon isotherms and breakthrough curves. *Water Res.* **2002**, *36*, 647–655.
(4) Haydar, S.; Garcia, M. A. F.; Utrilla, J. R.; Joly, J. R. Adsorption of p-nitrophenol on activated carbon with different oxidations. *Carbon* **2003**, *41*, 387–395.
(5) Podeh, M. R. H.; Bhattacharya, S. K.; Qu, M. Effects of nitrophenol on acetate utilizing methanogenic systems. *Water Res.* **1995**, *29*, 391–399.
(6) Pintar, A.; Levec, J. Catalytic oxidation of aqueous p-chlorophenol and p-nitrophenol solutions. *Chem. Eng. Sci.* **1994**, *49*, 439–4407.
(7) Aksu, Z.; Yener, J. A comparative adsorption/biosorption study of monochlorinated phenols onto various sorbents. *Waste Manage.* **2001**, *21*, 695–702.
(8) Koumanova, B.; Peeva-Antova, P. Adsorption of *p*-chlorophenol from aqueous solutions on bentonite and perlite. *J. Hazard. Mater.* **2001**, *90*, 229–234.
(9) Koumanova, B.; Kircheva, Z. Bentonite assisted bioprocess for 2-nitrophenol removal from wastewaters. *J. Univ. Chem. Technol. Metall.* **2003**, *38*, 71–78.
(10) Azanova, V. V.; Hradil, J. Sorption properties of macroporous and hyper-cross linked copolymers. *React. Funct. Polym.* **1999**, *41*, 163–175.
(11) Xu, Z. Y.; Zhang, Q. W.; Fang, H. H. P. Applications of porous resin sorbents in industrial wastewater treatment and resource recovery. *Crit. Rev. Environ. Sci. Technol.* **2003**, *33*, 323–389.
(12) Zhang, X.; Li, A.; Jiang, Z.; Zhang, Q. Adsorption of dyes and phenol from water on resin adsorbents: effect of adsorbate size and pore size distribution. *J. Hazard. Mater.* **2006**, *B137*, 1115–1122.
(13) Zhang, W.; Chen, J.; Pan, B.; Zhang, Q.; Zhang, B.; Wang, F. Synergistic interactions on phenol adsorption from aqueous solutions by polymeric adsorbents. *Chin. J. Polym. Sci.* **2005**, *23*, 441–447.
(14) Carmona, M.; Lucas, A. D.; Valverde, J. L.; Velasco, B.; Rodriguez, J. F. Combined adsorption and ion exchange equilibrium of phenol on Amberlite IRA-420. *Chem. Eng. J.* **2006**, *117*, 155–160.
(15) Ming, Z. W.; Long, C. J.; Cai, P. B.; Xing, Z. Q.; Zhang, B. Synergistic adsorption of phenol from aqueous solution onto polymeric adsorbents. *J. Hazard. Mater.* **2006**, *B 128*, 123–129.
(16) Crook, E. H.; McDonnell, R. P.; McNutty, J. T. Removal and recovery of phenols from industrial waste effluents with Amberlite XAD polymeric adsorbents. *Ind. Eng. Chem. Prod. Res. Dev.* **1975**, *14*, 113–118.
(17) Bhattacharyya, K.; Sharma, G. A. Kinetics and thermodynamics of Methylene Blue adsorption on Neem (*Azadirachta indica*) leaf powder. *Dyes Pigm.* **2005**, *65*, 51–59.
(18) Bhattacharyya, K. G.; Sharma, A. Adsorption characteristics of the dye, Brilliant green, on Neem leaf powder. *Dyes Pigm.* **2003**, *57*, 211–22.
(19) Boehm, H. P. *Adsorption by Carbons*; Elsevier: Amsterdam, 2008; pp 301−327.
(20) Hameed, B. H.; Tan, I. A. W.; Ahmad, A. L. Adsorption isotherm, kinetic modeling and mechanism of 2,4,6-trichlorophenol on coconut husk-based activated carbon. *Chem. Eng. J.* **2008**, *144*, 235–244.
(21) Langmuir, I. The constitution and fundamental properties of solids and liquids. *J. Am. Chem. Soc.* **1916**, *38*, 2221–2295.
(22) Freundlich, H. M. F. Uber die adsorption in losungen. *Phys. Chem.* **1906**, *57*, 385–471.
(23) Temkin, M. J.; Pyzhev, V. Kinetics of ammonia synthesis on promoted iron catalysts. *Acta Physicochem. URSS* **1940**, *12*, 217–256.
(24) Rivas, F. J.; Beltran, F. J.; Gimeno, O.; Frades, J.; Carvalho, F. Adsorption of landfill leachates onto activated carbon Equilibrium and kinetics. *J. Hazard. Mater.* **2006**, *B131*, 170–178.
(25) Redlich, O.; Peterson, D. L. A useful adsorption isotherm. *J. Phys. Chem.* **1959**, *63*, 1024–1026.
(26) Ng, J. C. Y.; Cheung, W. H.; McKay, G. Equilibrium studies of the sorption of Cu(II) ions onto chitosan. *J. Colloid Interface Sci.* **2002**, *255*, 64–74.
(27) McKay, G.; Blair, H. S.; Gardener, J. R. Adsorption of dyes on chitin I. Equilibrium studies. *J. Appl. Polym. Sci.* **1982**, *27*, 3043–3057.
(28) Ahmaruzzaman, M.; Sharma, D. K. Adsorption of phenols from wastewater. *J. Colloid Interface Sci.* **2005**, *287*, 14–24.
(29) León, C. A. L.; Solar, J. M.; Calemma, V.; Radovic, L. R. Evidence for the protonation of basal plane sites on carbon. *Carbon* **1992**, *30*, 797–811.
(30) Ho, Y. S.; McKay, G. Sorption of dye from aqueous solution by pit. *Chem. Eng. J.* **1998**, *70*, 115–124.
(31) Ho, Y. S.; McKay, G. Pseudo-second order model for sorption processes. *Process Biochem.* **1999**, *34*, 451–465.
(32) Giles, C. H.; MacEwan, T. H.; Nakhwa, S. N.; Smith, D. Studies in adsorption. Part XI. A system of classification of solution adsorption isotherms, and its use in diagnosis of adsorption mechanisms and in measurement of specific surface areas of solids. *J. Chem. Soc.* **1960**, 3973–3993.
(33) Khan, S. A.; Rehman, R.; Khan, M. A. Adsorption of Cr(III), Cr(VI) and Ag(I) on Bentonite. *Waste Manage.* **1995**, *15*, 271–82.
(34) Brennan, J. K.; Bandosz, T. J.; Thomson, K. T.; Gubbins, K. E.; Water in Porous Carbons-Review. *Colloids Surf., A* **2001**, *187−188*, 539–568.
(35) Aksu, Z.; Gönen, F. Biosorption of phenol by immobilized activated sludge in continuous packed bed: prediction of breakthrough curves. *Process Biochem.* **2004**, *39*, 599–613.

NOTE ADDED AFTER ASAP PUBLICATION

This paper was published ASAP on May 16, 2011. Citations throughout the paper were updated. The revised paper was reposted on May 27, 2011.